FLUORESCENCE LIFETIME CONTRAST COMBINED WITH PROBE MICROSCOPY

O. H. WILLEMSEN, O.F.J. NOORDMAN, F.B. SEGERINK
A.G.T. RUITER, M.H.P. MOERS & N.F. VAN HULST
Applied Optics group, Faculty of Applied Physics
& MESA Research Institute, University of Twente,
P.O.Box 217, 7500AE Enschede, the Netherlands.

ABSTRACT. Fluorescence lifetime imaging is combined with atomic force microscopy in an integrated scanning microscope using a silicon-nitride probe. The time decay of fluorescence is measured at each image position with a resolution of 50 ps by time correlated single photon counting using a frequency doubled mode-locked Ti-Sapphire laser and fast electronics. Images of a mixture of fluorescence labelled latex spheres are presented where the lifetime contrast of the different spheres can be directly correlated to the topography as detected by force microscopy.

1. Introduction

In Fluorescence Lifetime-resolved Imaging Microscopy (FLIM) [1] the temporal characteristics of luminescent emission in a fluorescence microscope image are recorded at each position in the image field [2]. Thus it is possible to measure directly the local mean lifetime of the emission and to discriminate among several fluorescent components in the image based on their distinct decay times.

The time decay of fluorescence is sensitive for environmental factors, which is mainly due to the lifetime of the excited state, typically 10 ns, long enough to involve processes with other molecules over 10 nm away at the moment of excitation. Thus photodynamic processes as molecular rotation, solvent and matrix relaxation, chemical reactions, quenching processes, singlet-triplet intersystem crossing, complex formation or energy transfer can all be studied best by their characteristic time dependence. Obviously mapping of the heterogeneity of the molecular environment in e.g. biological specimens is performed with higher selectivity by combining both temporal and spectral information.

The dynamic response of fluorophores can be measured using frequency domain or time domain methods. In the frequency domain the excitation is RF modulated (10 - 100 Mhz) and the phase shifted demodulated fluorescence response is measured [2, 3]. This phase fluorometry is a fast and efficient way to determine the mean fluorescence

M. Nieto-Vesperinas and N. García (eds.), Optics at the Nanometer Scale 223–233.

decay time, however for low signal levels approaching photon counting the method is not suitable. In the time domain the complete fluorescence decay curve is measured after excitation with a sub-ns pulse. Generally the time profile is determined using photon counting techniques and sampling over many excitation pulses. The acquisition of full decay curves over a total image is very slow, therefore often a compromise is chosen: instead of measuring the whole temporal profile the fluorescence is integrated over two pre-set time windows and the ratio of the integrated intensities is related to an average lifetime [4].

Currently the application of confocal FLIM arrangements is developing fast, especially in the biological domain. Yet ultimately diffraction sets a lower limit to the spatial resolution that can be obtained. Further improvement of resolution, while maintaining temporal optical contrast, requires measurement in the optical near-field using probe microscopy methods. Also the technique of Near-field Scanning Optical Microscopy (NSOM) has developed fast over recent years [5], including observation and spectroscopy of single molecules [6, 7]. Recently Dunn *et al.* [8] have demonstrated fluorescent lifetime measurements on photosynthetic membranes and Sunney Xie *et al.* [9] and Ambrose *et al.* [10] showed time resolved images of single molecules.

In this paper we present recent progress using an integrated set-up [11, 12] with simultaneous fluorescence lifetime imaging and atomic force microscopy.

2. Fluorescence lifetime

Upon irradiation with light close to the resonance for the singlet $S_0 \Rightarrow S_1$ transition molecules are excited within about 10 fs to one of the vibrational state of S_1. The processes competing with the subsequent fluorescence are inter-system crossing (ISC) to the triplet manifold, internal conversion (IC) to the ground state and dissociation (D) through a photochemical reaction. Vibrational relaxation to the lowest vibrational level of S_1 occurs on ps time scale and is generally complete before electronic relaxation. The subsequent radiative decay rate k_R depends on the overlap of the molecular orbitals for the electron in S_0 and S_1. The value of k_R extends from 10^9 s^{-1} for fully allowed transitions ($\pi\pi^*$ in common dye molecules) to 10^7 s^{-1} for symmetry forbidden transitions (aromatic molecules) down to 10^5 s^{-1} ($n\pi^*$, e.g. carbonyl compounds). Due to the competing decay channels (ISC, IC, D) the effective fluorescence decay time τ_F is shorter than k_R^{-1},

$$\tau_F = (k_R + k_{ISC} + k_{IC} + k_D)^{-1}$$

The observed fluorescence decays exponentially with the effective decay time τ_F. However due to the existence of several decay channels in practise often a more complex (bi-exponential) decay is observed. The quantum yield Φ_F for fluorescence is $k_R \cdot \tau_F < 1$, typically 0.5 - 0.9 . Thus it is clear that, even without interaction with the environment, the amount of fluorescence depends on the size of the radiative rate constant k_R relative to the sum of all rates (Σk). For optimum signal in a fluorescence experiment fluorophores with dominant radiative decay (10^8 - 10^9 s^{-1}) and quantum yield close to unity have to be chosen.

3. Time correlated single photon counting

Temporal profiles of the fluorescence decay are recorded using Time Correlated Single-Photon Counting (TCSPC) [13, 14]. The basic electronic scheme is given in figure 1.

Optical excitation pulses are generated from a mode-locked Ti:Sapphire laser (Spectra-Physics, Tsunami 3960), which gives 80 fs pulses in the wavelength region 700-1100 nm at a repetition rate of 82 MHz. After frequency doubling pulses in the region 350-550 nm are delivered every 12.2 ns. A sample is illuminate and the generated fluorescence is detected with a fast sensitive detector: a MicroChannel Plate PhotoMultiplier Tube (MCP-PMT, Eldy EMI-132/300), which allows detection of single photons and gives reproducible electric pulses with a width of 420 ps. Part of the direct laser pulse is detected by a fast photo-diode (BPX65). Both MCP signal and photo-diode signal are amplified (EG&G Ortec VT120 & 9306) and discriminated. Hereto constant fraction discriminators (EG&G Ortec 935) are used, which enable exact timing of the pulse maximum with an accuracy only limited by the jitter and noise of the pulse. The discriminated pulses act as start and stop pulses for a Time-to-Amplitude Converter (TAC, EG&G Ortec 566). The central part of the TAC is a capacitor that starts to charge up at the moment the start pulse arrives and ends charging up by the arrival of a stop pulse. Thus a pulse is generated at the output of the TAC with an amplitude proportional to the time difference between start and stop pulse. The pulses are stored in a multichannel analyzer. Every laser shot that generates a fluorescent photocount starts the TAC and gives an output pulse. With repetitive pulses a histogram of the time difference distribution builds up. Of course TCSPC is based on zero or one photon per laser pulse. As a consequence the fluorescent photon emission rate is limited to ~ 1% of the laser repetition rate, i.e. 10^6 photons/s. In practise the maximum count rate is further limited to $5 \cdot 10^4$ counts/s by the A/D conversion in the multi-channel analyzer.

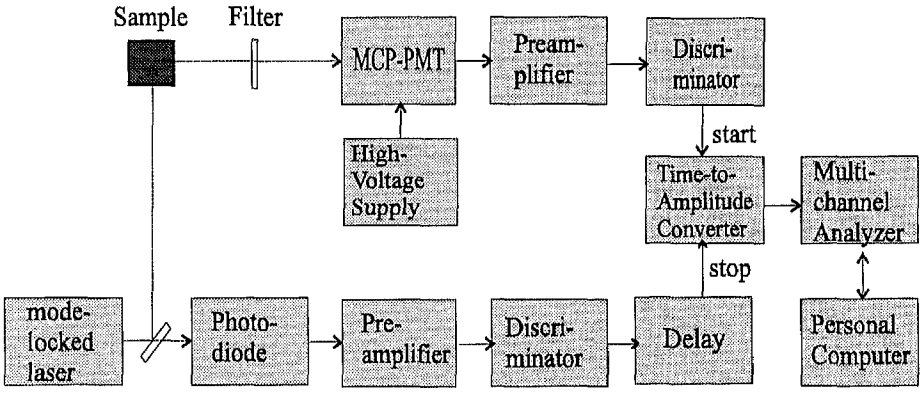

Figure 1: Detection electronics for Time Correlated Single Photon Counting.

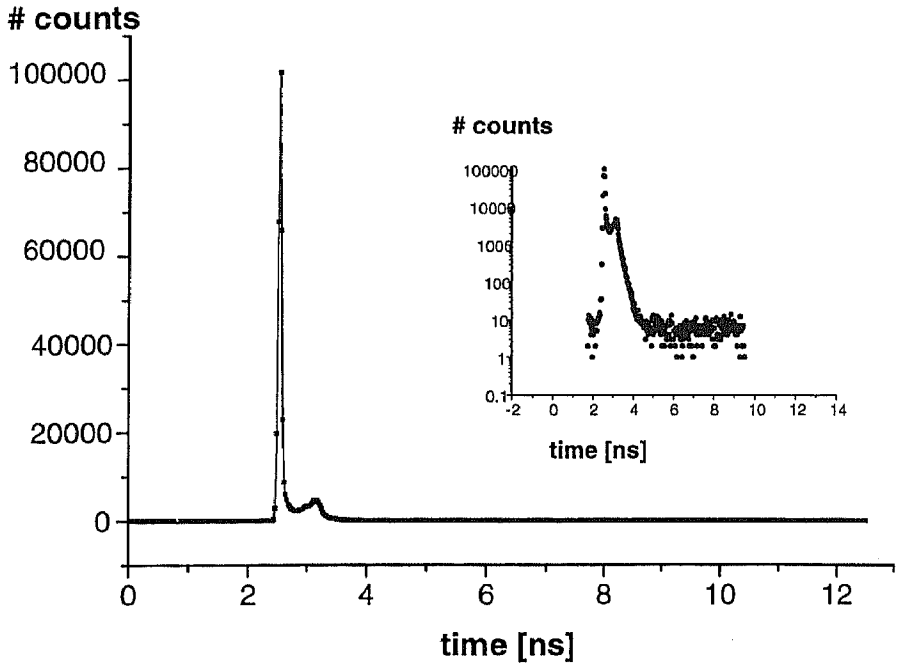

Figure 2: System response function with FWHM = 70 ps; inset log-scale.

The measured temporal intensity profile $I_F(t)$ will be a convolution of the actual profile $G(t)$ and the system response function $P(t)$, as given by

$$I_F(t) = \int_0^t P(t')G(t-t')dt' .$$

If the instrument response function is sufficiently narrow compared to the fluorescence lifetime no deconvolution is necessary. The instrumental function is determined by the combination of laser, detector and electronics and has been tested for its impulse response, as plotted in figure 2. The system response function has a peak of 70 ps FWHM and 140 ps at the 10% level. The main peak is followed by a broader second peak with a 22× lower signal at 610 ps delay, caused by the discriminator action.

Due to the 12.2 ns repetition period of the laser and partial overlap of the start pulse with previous stop pulses in practise a time window of 8 ns is available. The maximum lifetime to be determined is about 4 ns if one requires two decades of fluorescence decay for a sufficient exponential fit.

4. FLIM - AFM set-up

The microscopic set-up is a modified version of a combined NSOM/AFM [15] as described by Ruiter *et al.* [16]. The sample is scanned using a large area 200 x 200 μm piezo-electric scanner. A SiN integrated probe and an optical beam deflection system constitute the AFM part. Two large working distance objectives (0.55 NA) are arranged confocally with two pinholes to form the FLIM part. The Ø 1 μm focus on the sample area is ~ 4 μm shifted relative to the AFM probe. An additional Hg-lamp and CCD camera facilitate alignment of AFM and FLIM and allow direct viewing of the sample area of interest. At each x-y position of the scanner 3000 photocounts are collected in a histogram of 64 bins, yielding a time profile for each image pixel.

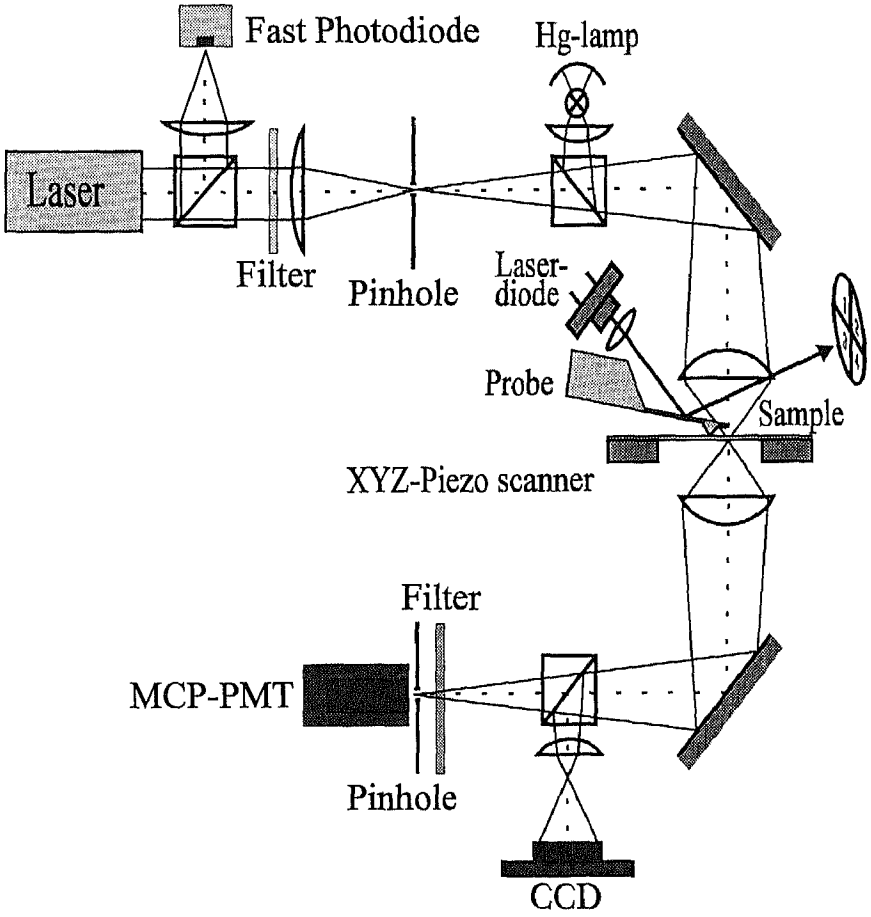

Figure 3: Combined Fluorescence Lifetime Imaging Microscope and Atomic Force Microscope (FLIM - AFM).

5. Measurements and Discussion

5.1. MEASUREMENTS ON FLUORESCENT MOLECULES IN SOLUTION.

The fluorescent molecules Streptavidin PE (Becton & Dickinson, Streptavidin PhcoErythyn) and F18 (fluorescein isothiocyanate, FITC, coupled to 18 carbon atoms), both in PBS (Phosphate Buffer Saline) at pH = 7.37, were used for lifetime measurement. The molecules are excited at 485 nm and 460 nm, respectively. Figure 4 shows a typical fluorescence time profile for F18. The exponential decay shows some oscillations caused by the electronics. The decay curves are fit to a single exponential decay, taking into account an offset due to the darkcounts of the MCP. Comparison of the determined lifetimes to literature values in table 1 shows good agreement.

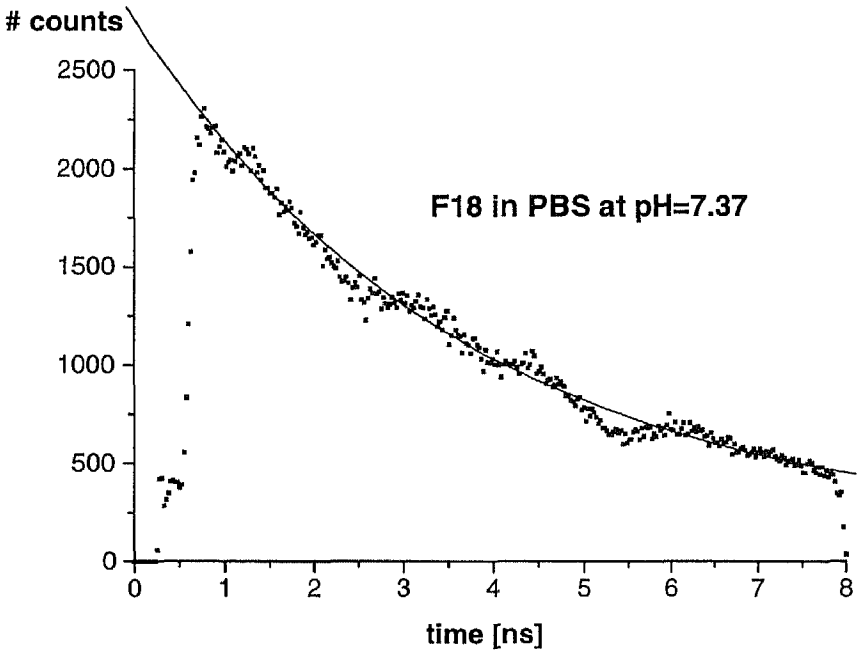

Figure 4: Fluorescence decay of F18 in PBS at pH=7.37 with 460 nm excitation.

Fluorophore	Exp., with / without offset [ns]	Literature [ns]
Streptavidin PE	3.2 / 3.3	2.9 / 3.2 [17]
FITC/F18	3.7 / 4.3	4.2 [18], 3.8 [19]

Table 1: Experimental an literature fluorecence lifetimes.

5.2. MEASUREMENTS ON FLUORESCENTLY STAINED BEADS

A mixture of two kinds of fluorescence labelled latex spheres was prepared differing both in size and time-resolved behaviour was prepared: 70% 1.0 μm beads stained with fluorescein and 30% 1.8 μm beads (both Polysciences). The fluorescence decay of the separate spheres was measured, both in water and on glass. Figure 5 shows decay curves, where the profile of the 1.8 μm beads is multiplied by 3 for clarity. The 1.0 μm beads display a single exponential decay with 2.4 ns lifetime. The 1.8 μm beads show a fast and a slow component in the decay, with 600 ps and 3.0 ns lifetime, respectively, while the average single exponential decay time is 1.6 ns.

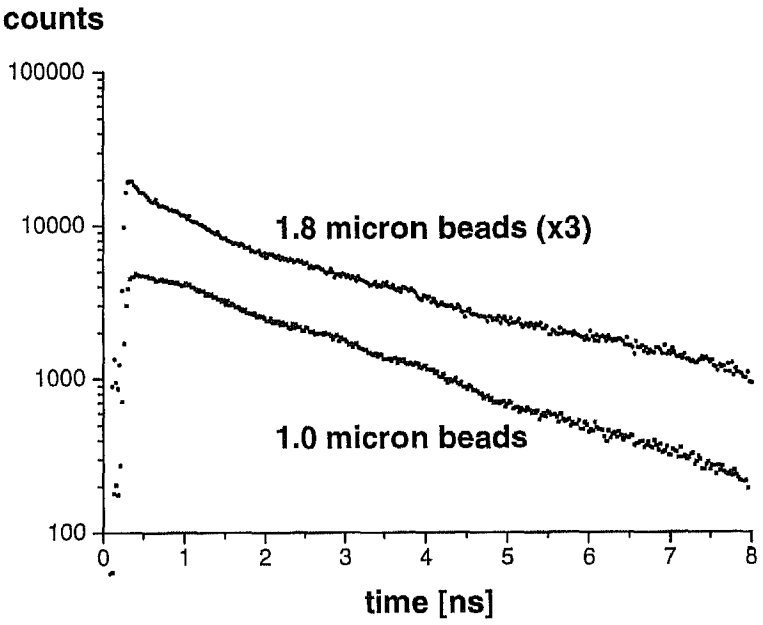

Figure 5: Fluorescence decay 1.8 μm and 1.0 μm labelled beads

5.3. COMBINED FLUORESCENCE LIFETIME AND FORCE MICROSCOPY.

For microscopic imaging a droplet of the mixed beads was put on an object glass and slightly heated to fix the spheres to the glass. Thus monolayers and multilayers of closely packed mixed spheres are fabricated. The sample is illuminated at 480 nm of the frequency doubled Ti:Sapphire laser to excite both fluorophores. While scanning the sample time profiles and AFM signal are recorded simultaneously for each pixel. The offset AFM probe and laser focus have sufficient overlap within a 30 x 30 μm scan area to allow comparison. Images at different time windows were extracted from the data and plotted together with the AFM scan in figures 6 and 7.

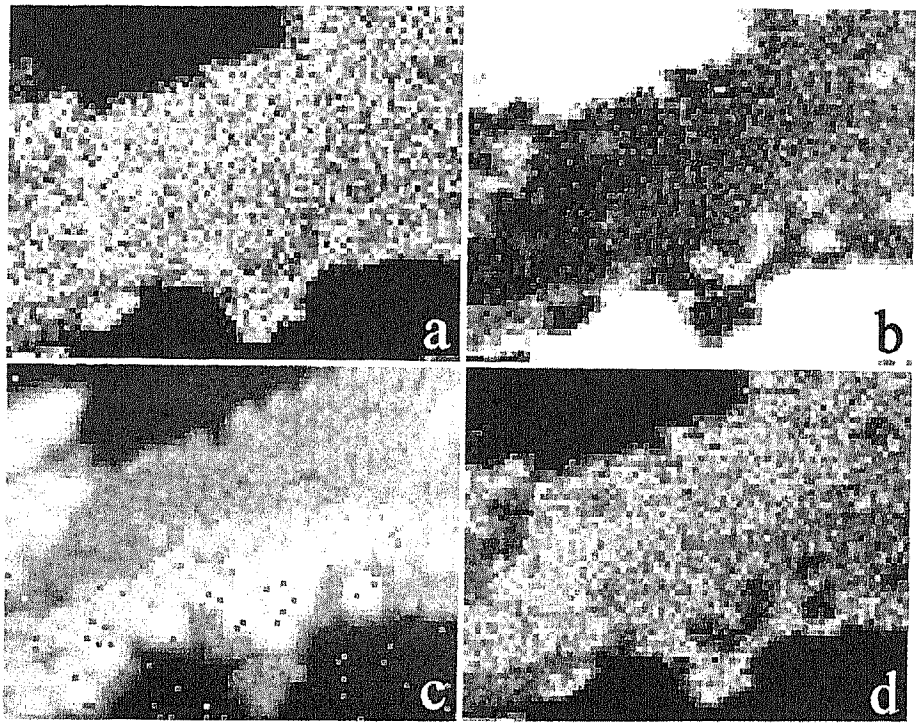

Figure 6:

30 x 22 μm image of a mixture of two types of fluorescence labeled latex spheres on glass: 1.8 μm and 1.0 μm:
(a) Fluorescence signal in the first 400 ps after excitation.
(b) Fluorescence signal in 3.1 - 7.0 ns interval after excitation.
(c) Simultaneously recorded atomic force image.
(d) Ratio image of fast over slow fluorescence.

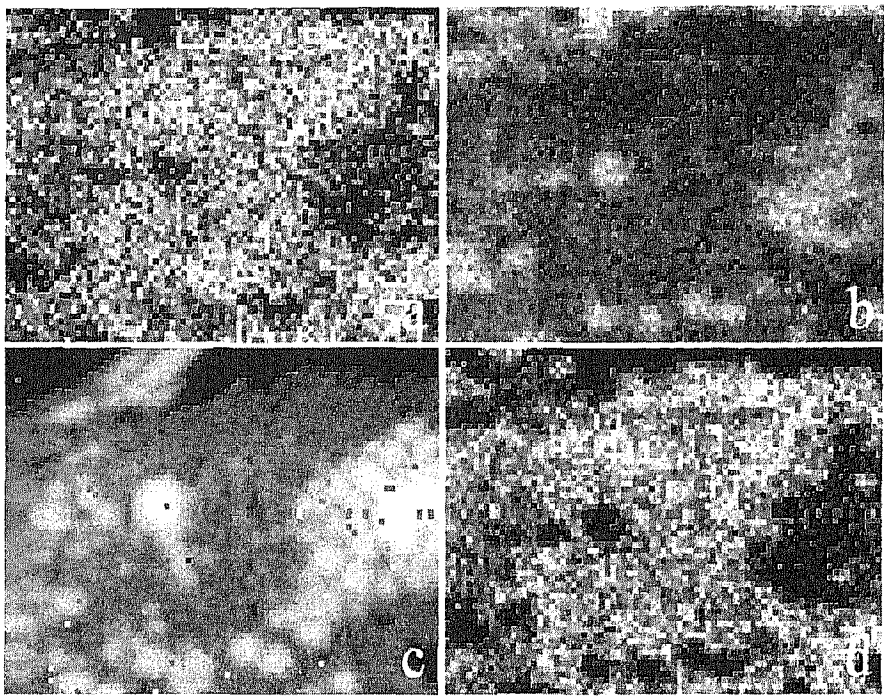

Figure 7:

30 x 22 μm image of a mixture of two types of fluorescence labeled latex spheres on glass: 1.8 μm and 1.0 μm:
(a) Fluorescence signal in the first 780 ps after excitation.
(b) Fluorescence signal in 3.1 - 7.0 ns interval after excitation.
(c) Simultaneously recorded atomic force image.
(d) Ratio image of fast over slow fluorescence.

In figures 6 and 7 image (a) shows the fast fluorescence signal in the first few 100 ps, while image (b) shows the long term fluorescence in the 3.1 - 7.0 ns time interval. Comparison clearly shows the contrast reversal: the small spheres dominate in the first ns and the slow component of the larger beads dominates on the longer timescale of several ns. It should be noted that at each pixel 3000 counts are stored and consequently the images show the relative contrast for the given time interval. The corresponding topographic AFM images in (c) show the glass substrate with monolayers and sometimes double layers of 70% small beads and 30% large beads. Finally in (d) images are presented of the ratio of fast over slow fluorescence, which show enhanced contrast compared to the time window images. The discrimination of the spheres on size in the AFM images corresponds well to the time contrast in the FLIM images. In figure 6c a monolayer to double layer step of small beads is observed while the lifetime is unchanged in figure 6d. On an additional layer with large beads the lifetime does change, as expected. Some structures in the AFM image are non-fluorescent and do not show up in the optical images.

6. Conclusions

A combined FLIM - AFM set-up has been presented. Fluorescence lifetime images have been obtained simultaneously with topographic AFM images. The time resolution is determined by a system response function of 70 ps FWHM. Lifetimes of 1-4 ns can be determined. Lifetimes of 3.3 and 3.7 ns have been determined for Streptavidin PE and F18, respectively. The spatial resolution of the optical system is about 600 nm, as determined by the numerical aperture of the objectives. The lateral resolution of the AFM is determined by tip sharpness and drift during time integration for fluorecence detection. Different fluorescent beads have been discriminated on fluorescence lifetime characteristics in good correspondence with the discrimination on size.

The time window for detection can be extended using a pulse picker for the mode-locked laser, which allows measurement of longer lifetimes.

The optical resolution will be further improved in a near-field optical arrangement using a metal-coated fibre probe or an integrated NSOM probe [16]. Thus the nano-environment of fluorophores will be analyzed by the photo-dynamic response.

7. Acknowledgements

The authors thank Thomas Widén, Patrik Reimer, Kees van der Werf, John van Noort, Bart de Grooth and Cees Otto for their contributions and suggestions. This research is mainly supported by the Dutch Foundation for Fundamental Research (FOM, division Atomic Physics & Quantum Electronics) and the European network on Near-field Optics and Nanotechnology.

8. References

1. Gadella, T.W., Jovin, T.M. and Clegg, R.M. (1993) Fluorescence lifetime imaging microscopy (FLIM): spatial resolution of microstructures on the ns time scale, *Bioph. Chem.* **48**, 221-239.
2. Lakowicz, J.R. and Berndt, K.W. (1991) Lifetime-selective fluorescence imaging using an RF phase sensitive camera, *Rev. Sci. Instrum.* **62**, 1727-1734.
3. Laczko, G., Gryczynski, I., Gryczynski, Z., Wiczk, W., Malak, H. and Lakowicz, J.R. (1990) Phase fluorometry. *Rev. Sci. Instrum.* **61**, 2331.
4. Buurman, E.P., Sanders, R., Draaijer, A., Gerritsen, H.C., van Veen, J.J.F., Houpt, P.M. and Levine, Y.K. (1992) Fluorescence lifetime imaging using a confocal laser scanning microscope, *Scanning* **14**, 155-159.
5. Betzig, E. and Trautman, J.K. (1992) Near-field optics: microscopy, spectroscopy and surface modification beyond the diffraction limit, *Science* **257**, 189-195.
6. Betzig, E. and Chichester, R.J. (1993) Single Molecule observed by Near field Scanning Optical Microscopy, *Science* **262**, 1422-1425.
7. Trautman, J.K., Macklin, J.J., Brus, L.E. and Betzig, E. (1994) Near field spectroscopy of single molecules at room temperature, *Nature* **369**, 40-42.
8. Dunn, R.C., Holtom, G.R., Mets, L. and Sunney Xie, X. (1994), Near-field fluorescence imaging and fluorescence lifetime measurement of light harvesting complexes in intact photosynthetic membranes, *J. Phys. Chem.* **98**, 3094-3098.
9. Sunney Xie, X. and Dunn, R.C. (1994) Probing Single Molecule Dynamics, *Science* **265**, 361-364.
10. Ambrose, W.P., Goodwin, P.M., Martin, J.C. and Keller, R.A. (1994) Alterations of Single Molecule Fluorescence Lifetimes in Near-Field Optical Microscopy, *Science* **265**, 364-367.
11. Van Hulst, N.F., Moers, M.H.P., Noordman, O.F.J., Faulkner, T., Segerink, F.B., van der Werf, K.O., De Grooth B.G. and Bölger B. (1992) Operation of a Scanning Near field Optical Microscope in reflection in combination with a scanning force microscope, *SPIE* **1639**, 36-43.
12. Moers, M.H.P., Tack, R.G., Van Hulst, N.F. and Bölger, B. (1994) Photon scanning tunneling microscope in combination with a force microscope, *J. Appl. Phys.* **75**, 1254-1257.
13. O.Connor, D.V. and Philips, D. (1984) Time correlated single photon counting, Academic Press, London,
14. Wilkerson, C.W. Goodwin, P.M., Ambrose, W.P., Martin, J.C. and Keller, R.A. (1993) Detection and lifetime measurement of single molecules in flowing sample streams by laser-induced fluorescence, *Appl. Phys. Lett.* **62**, 2030-2032.
15. Van Hulst, N.F., Moers, M.H.P. and Bölger, B. (1993) Near-field optical microscopy in transmission and reflection modes in combination with force microscopy, *J. Microscopy.* **171**, 95-105.
16. Ruiter, A.G.T., Moers, M.H.P., Jalocha, A. and van Hulst, N.F. (1995) Development of an integrated NSOM probe. *Ultramicroscopy* **58**, in press.
17. Grabowski, J. and Gantt, E. (1978) *Photochemistry and Photobiology* **28**, 39.
18. Chen, R.F.(1969) *Archives of Biochemistry and Biophysics* **133**, 263
19. Haughland, R.P. (1992) Handbook of fluorescent probes and research chemicals, 5th ed., Molecular Probes Inc. Eugenen, Oregon.